Solar and Interplanetary Signatures of a Maunder-like Grand Solar Minimum around the Corner - Implications to Near-Earth Space

P. Janardhan[1], Susanta Kumar Bisoi [2], S. Ananthakrishnan[3], R. Sridharan[4], L. Jose[4]

[1] Physical Research Laboratory, India.
[2] National Astronomical Observatories, Chinese Academy of Sci., Beijing China
[3] Department of Electronic Science, University of Pune, India
[4] Space & Atmospheric Sciences Division, Navrangpura, Ahmedabad, India.

E mail (jerry@prl.res.in, susanta@nao.cas.cn, subra.anan@gmail.com, sridharan@prl.res.in).

Accepted : 28 August 2015

Abstract Our study of a steady decline of solar high-latitude (≥45°) photospheric magnetic fields for the past 20 years combined with the fact that cycle 24 is already past its peak, implies that high-latitude fields are likely to decline until ~2020, the expected minimum of cycle 24.Also, interplanetary scintillation (IPS) observations, at 327 MHz, of solar wind micro-turbulence levels during 1983—2013, have shown a steady decline, in sync with the declining solar high-latitude fields. An estimateof both the heliospheric magnetic field (HMF) strength in 2020 and the floor value of the HMF, using the correlation between the polar field and the HMF at solar minimum, was found to be 4.0 (±0.6) nT and 3.2 (±0.4) nT, respectively. Using the estimated value of the HMF in 2020, the peak sunspot number for solar Cycle 25 was estimated to be 69 (±12). These results and the fact that solar magnetic fields continue to decline at present, begs the question as to whether we are headed towards a long period of very low sunspot activity similar to the well known Maunder minimum between 1645-1715. An assessment of possible impact of such a likely grand minimum on terrestrial ionospheric current systems, based on the one-to-one correlation of sunspot number and night time F-region maximum electron density, reveals that the period post 2020 will be useful for undertaking systematic ground based low-frequency radio astronomy observations, as the night time ionospheric cutoff-frequency could be well below 10 MHz.

Keywords Sun: activity, Sun: photosphere, solar wind, solar – terrestrial relations

1. Introduction

Sunspots or dark regions of strong magnetic fields on the sun are generated via magneto-hydrodynamic processes involving the cyclic generation of toroidal, sunspot fields from pre-existing poloidal fields and their eventual regeneration through a process, referred to as the solar dynamo Charbonneau (2010). This leads to the well known periodic 11-year solar cycle of waxing and waning sunspot numbers. However studies of past sunspot activity reveals periods like the Maunder minimum (1645—1715) when the sunspot activity was extremely low or virtually non-existent. Using ^{14}C records from tree rings going back 11, 000 years in time, 27 such prolonged or grand solar minima have been identified Usokin et al. (2007), implying that conditions existed in these 17% - 18% of solar cycles that forced the sun into grand minima. The current solar cycle 24 was preceded by one of the deepest solar minima in the past 100 years, with sunspot numbers continuously remaining well below 25, and thereby causing cycle 24 to start ~1.3 years later than expected Jian et al. (2011). Also solar cycle 24, with a peak smoothed sunspot number ~75 in November 2013, has been the weakest since cycle 14 in the early 1900's.

Our recent studies of solar photospheric magnetic fields, using synoptic magnetograms from the National Solar Observatory (NSO), Kitt Peak (NSO/KP), between 1975—2010, spanning the last three solar cycles, have shown a steady decline in solar photospheric magnetic fields at helio-latitudes (≥45°) until 2010, with the observed decline having begun in the mid-1990's Bisoi et al. (2014b). Also, recent studies Livingston et al. (2012) of the sunspot umbral field strengths have shown that it has been decreasing by ~50 G per year. It is known that for field strengths below about 1500 G, there would be no contrast between the photosphere and sunspot regions, thereby making the later invisible Livingston et al. (2012). These authors claimed that the umbral field strengths in cycle 25 would be around 1500 G, and thus there would be very little/no sunspots visible on the solar photosphere.

Studies of the heliospheric magnetic fields (HMF), using in-situ measurements at 1 AU, have also shown a significant decline in their strength (Smith and Balogh,

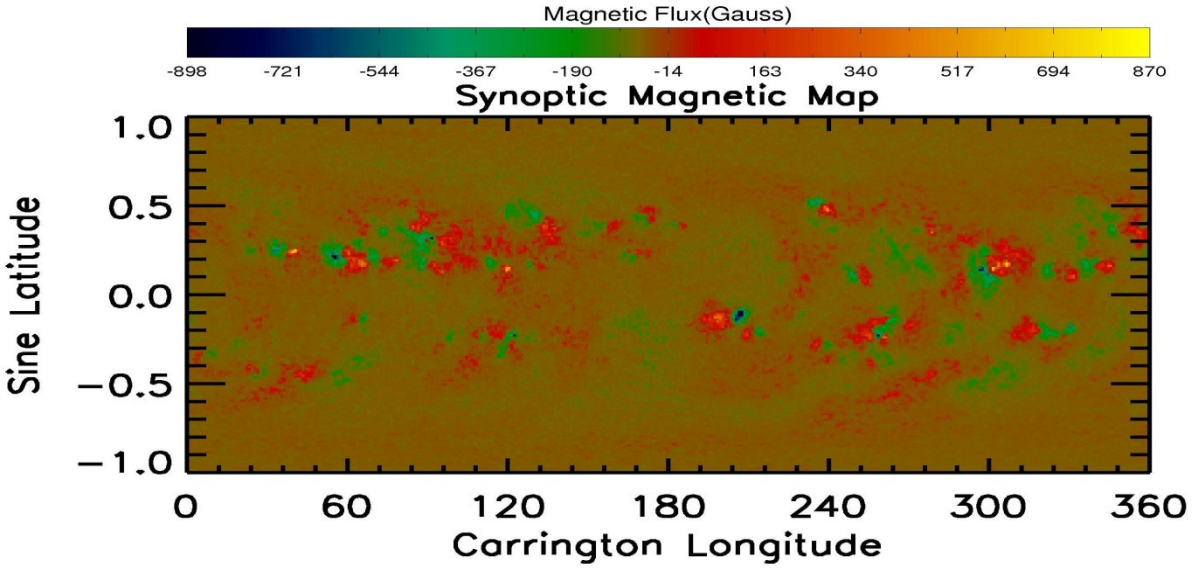

Figure 1 A Carrington rotation synoptic map, in the form of sine of latitude and longitude, depicting the photospheric distribution of magnetic fluxes. The color bar at the top indicates the strength of magnetic flux in units of G.

2008; Wang et al., 2009; Connick et al., 2011; Cliver and Ling, 2011). In addition, using 327 MHz observations from the four station IPS observatory of the Solar-Terrestrial Environment Laboratory (STEL), Nagoya University, Japan, we have examined solar wind micro-turbulence levels in the inner-heliosphere and have found a similar steady decline, continuing for the past 18 years, and in sync with the declining photospheric fields Janardhan et al. (2011). A study, covering solar cycle 23, of the solar wind density modulation index, $\epsilon_N \equiv \Delta N/N$, where, ΔN is the rms electron density fluctuations in the solar wind and N is the density, has reported a decline of around 8%, Bisoi et al. (2014a) which the authors attributed to the declining photospheric fields.

In light of the very unusual nature of the minimum of solar cycle 23 and the current weak solar cycle 24, we have re-examined in this paper, solar photospheric magnetic fields between 1975—2013, the HMF between 1975—2014, and the solar wind micro-turbulence levels between 1983—2013. We aim to estimate the peak sunspot number of solar cycle 25, and address whether we are heading towards a grand minimum much like the Maunder minimum.

The cyclic magnetic activity of the Sun, manifested via sunspot activity, modulates the heliospheric environment, and the near-Earth space. It is therefore imperative that we examine how the recent changes in solar activity should have influenced the near-Earth space environment. We have therefore also examined the response of the Earth's ionosphere, for the period 1994—2014, to assess the possible impact of such a Maunder-like minimum on the Earth's ionospheric current system.

2. Photospheric Magnetic Fields

For photospheric magnetic fields, we used mainly ground-based synoptic magnetograms from the National Solar Observatory (NSO), Kitt-Peak (NSO/KP), USA, covering Carrington Rotations (CR) CR1625—CR2151, for the period (February 1975) 1975.14—(July 2014) 2014.42. NSO/KP magnetograms are freely available in the public domain as standard Flexible Imaging Transport System (FITS) files in the sine of latitude and longitude format of 180 × 360 arrays. Figure 1 shows one such CR synoptic magnetogram which depicts the photospheric distribution of magnetic fluxes. The positive and negative magnetic fluxes are shown in red and green respectively, while the color bar at the top indicates the strength of magnetic flux in units of Gauss (G).

Different groups of researchers have considered different solar latitude ranges to represent solar polar fields, and they have estimated them by averaging the magnetic flux in a defined high-latitude polar zone. Till date however, the polar area considered has been arbitrary Upton and Hathaway (2014). For example, Wilcox Solar Observatory (WSO) polar fields are those at latitudes ≥ 55°. Other researchers have used the area above latitudes ≥ 60° de Toma (2011) and still others have used the area above latitudes ≥ 70° Munoz-Jaramillo et al. (2012) to represent polar or high latitude fields. For the present study, we have considered photospheric magnetic fields in the latitude range 45^0-78^0 as representative of polar fields, referred to in the rest of the paper as high-latitude fields. We have estimated photospheric magnetic fields, from synoptic magnetograms, by using longitudinal

averages of the whole 360° array of Carrington longitudes to produce 1° strips of data for each CR of 27.275 days. High-latitude fields, in the range 45° - 78°, were then computed by appropriate averaging (Janardhan et al., 2010; Bisoi et al., 2014b).

Figure 2 shows the signed values of the high-latitude fields for the Northern (red) and Southern (blue) hemispheres, for solar cycles 21, 22, 23, and 24. The curves show the variation of the smoothed magnetic field and the asymmetric polar reversal between the hemispheres in each of the Solar Cycles 21-24. It may be noted that the occurrence of magnetic field reversal in both the hemispheres in Cycle 24 indicates that the ongoing solar Cycle 24 is past its peak and that the declining phase of the cycle has begun.

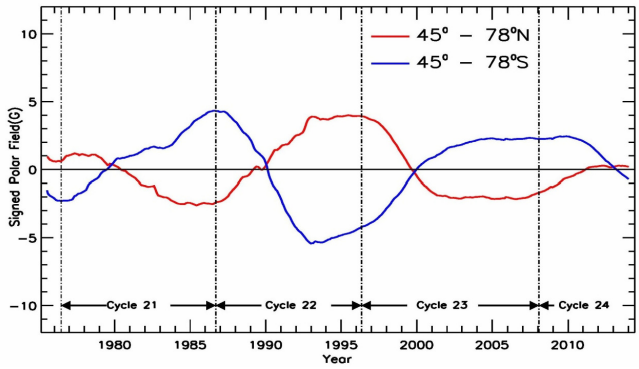

Figure 2 The smoothed signed photospheric magnetic fields in the latitude range 45°-78° for the Northern (red) and Southern (blue) hemispheres for solar cycles 21, 22, 23, and 24.

Figure 3 plots the temporal variations of the derived photospheric field strengths showing a steady decrease for past 20 years, from ~1995. It must be borne in mind here that the high-latitude fields described here are the absolute value of the field in the latitude range 45° - 78° and not the signed value of the field which normally reverses or goes through zero, as shown in Figure 2, at every solar maximum. This is commonly referred to as polar reversals. In Figure 3, the declining trend in the photospheric fields are seen to continue after the slight increase during the period 2010 - 2011. A close inspection of the behavior of the high-latitude fields in Cycles 21, 22, and 23 from Figure 3 shows that they normally decline after the solar maximum until the next solar minimum. The current solar cycle 24 is now past its maximum and the field strength is likely to continue to decline at least until 2020, the minimum of the current Cycle 24, indicated in Fig. 3 by a dashed red vertical line. Thus, the steady decline which started in ~1995 is expected to go on for a period of ~24 years. The solid red line in Fig. 3 is a best fit to the annual means, for the period 1994.48-2014.42, while the dotted red line is an extrapolation of the best fit line up to 2020. The least square fit shown in Fig. 3 is statistically significant (Pearson's correlation coefficient, r = -0.91, significance level = 99%) and the extrapolation implies the expected field strength is likely to drop to ~1.8 G by 2020, the expected minimum of the current solar cycle 24, shown in Figure 3 by a vertical red dashed line. In Fig. 3, the black horizontal, dotted line, is drawn at a value of 1.8 G. It may be noted here that sunspot numbers in the present cycle 24, up to early 2013, are comparable to the sunspot records during the Dalton minimum, which began in Cycle 5 and continued until Cycle 7 (Goelzer et al., 2013; Zolotova and Ponyavin, 2014). These authors went on to predict sunspot numbers for the next 10 years from 2013 to 2022, computed using sunspot records during the Dalton minimum from the year 1805 onward. The sunspot prediction (see Fig. 5 in Goelzer et al. (2013)) showed that the coming solar minimum of cycle 24 is expected to occur in 2020. We have therefore, in this study, taken 2020 to represent the expected year of solar minimum for the ongoing solar cycle 24.

The high-latitude fields, above latitudes of 45°, used in the paper are mainly confined to solar latitudes, where sunspots generally don't appear. However, it may be noted that solar dynamo models used to explain the solar activity cycle start with the assumption of a pre-existing poloidal field at the start of a cycle. This pre-existing field is transformed to a toroidal field within the sun and appears years later during the maximum phase as the sunspot field. It is also known that the sun's polar field serves as a seed for future solar activity through their transportation by an equator ward subsurface meridional flow Petrie (2012). As a result, polar fields act as an important and crucial input in predicting the strength of future solar cycles (Schatten and Pesnell, 1993; Schatten, 2005; Svalgaard et al., 2005; Choudhuri et al., 2007). Our studies of photospheric fields, confined to high-latitudes ≥ 45°, have shown a steady declining trend for ~20 years, in their (absolute field) strength. As mentioned earlier, since solar cycle 24 is already past its peak, the field strength is likely to continue to decline until 2020, by which time the field strength is likely to be ~ 1.8 G and the period of continuous decline will be 25 years, or greater that a full magnetic cycle of 22 years. Such continuously weak high-latitude fields would imply that the toroidal field strengths will also be weak and produce weak sunspot fields in subsequent cycles.

3. The Heliospheric Magnetic Field

Svalgaard and Cliver (2007), using a study of heliospheric magnetic fields (HMF) based on measurements of geomagnetic indices from 1872-2004, had proposed a floor level for the HMF of ~4.6 nT.

According to these authors, the floor is basically the annual average value to which the HMF strength approaches at each solar minimum. However, during the last protracted solar minimum of Cycle 23, measurements of the HMF at 1 AU have shown a significant decline in the HMF strength going well below 4.6 nT. This prompted a revision in the floor level of the HMF Cliver and Ling (2011) based on two independent correlations. The first was by using a correlation between the dipole moment and the HMF at Cycle minimum, while the second was by using a correlation between the HMF at each Cycle minimum and the yearly sunspot number at the maximum of the following Cycle. These authors reported a revised floor level of 2.8 nT and suggested that the floor of the HMF is due to the constant baseline open flux from the slow solar wind, and the always present small-scale magnetic fields on the Sun are presumably the source of slow solar wind flows. A similar study, using a correlation between the calibrated database of polar magnetic flux and the HMF from the OMNI data base, Munoz-Jaramillo et al. (2012) have reported a floor level of the HMF of 2.77 nT.

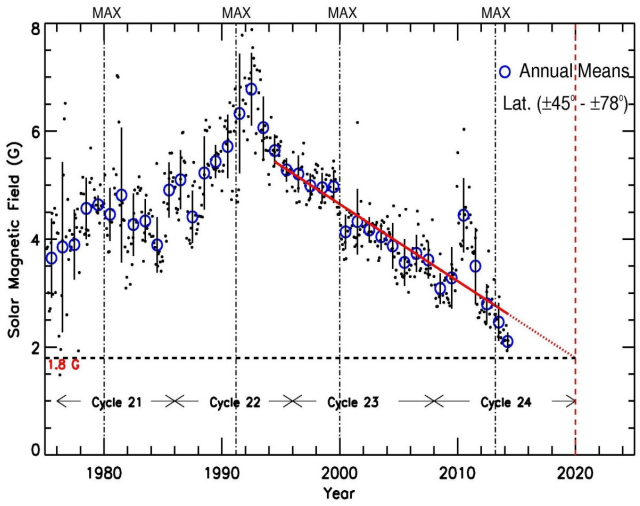

Figure 3 Photospheric magnetic fields in the latitude range 45°-78°, computed from the NSO/KP magnetograms, for the period of 1975.14-2014.42. While the solid filled dots are actual measurements of magnetic fields, the open blue circles are annual means with one sigma error bars. The solid red line is a best fit to the declining trend of the annual means, while the dotted red line is an extrapolation of the best fit line until 2020, indicated by a dashed red vertical line. The horizontal dashed line is marked at 1.8 G, the expected field strength in 2020. The vertical dotted lines are marked at the respective solar maximum of Cycles 21, 22, 23, and 24.

Based on the aforementioned studies of a correlation between polar flux and HMF at solar minimum (Cliver and Ling, 2011; Munoz-Jaramillo et al., 2012), and the fact that the surviving polar fields actually determine the floor level of the HMF Wang and Sheeley (2013), we have revisited the floor level in the HMF using it's correlation with the unsigned high-latitude photospheric fields. It is to be noted that studies mentioned earlier used the signed polar flux (or the dipole moment estimated from the signed polar fields). Photospheric magnetic fields used were computed from NSO/KP synoptic magnetograms for the period 1975.14-2014.42 and covering Carrington Rotations (CR) CR1625-CR2151.

The upper panel of Figure 4 shows (filled black circles) measurements of the 27-day averaged values of HMF and (open blue circles) annual means of HMF with 1 σ error bars between 1975-2014, obtained using data, at 1 AU, from the OMNI2 database. The horizontal dotted line is marked at the proposed floor value of the HMF of 4.6 nT, Svalgaard and Cliver (2007), while the vertical grey bands demarcate 1 year intervals Wang et al. (2009) around the minima of solar cycles 20, 21, 22 and 23 corresponding to CR1642-1654, CR1771-1783, CR1905-1917, and CR2072-2084, respectively. Average values of the high latitude (45°-78°) fields were computed in these 1 year intervals for the period 1975-2014 using NSO/KP synoptic magnetograms. The lower panel of Figure 4 shows the correlation between the high latitude or polar field (B_p) and the HMF (B_r) obtained using values for both B_p and B_r for 1 year intervals around the minima of cycles 20, 21, 22 and 23, demarcated in Figure 4 (upper panel) by grey vertical bands. It is evident from Figure 4 (upper panel) that the HMF has declined well below the proposed floor level of 4.6 nT, and has reached ~3.5nT during the minimum of Cycle 23. A linear least square fit to the data, with a Pearson's correlation coefficient of r=0.54 at a significance level of 99%, gave a value of the HMF of B_r = 3.2±0.4 nT, when B_p = 0 as shown in equation 1.

$$Br = (3.2 \pm 0.4) + (0.43 \pm 0.09) \times Bp \qquad (1)$$

This implies that even if the polar field, B_p drops to zero or to very low values, the HMF will persist at a floor level of 3.2±0.4 nT. From Fig. 3 it can be seen that the high latitude field drops to be 1.8 ± 0.08 G in 2020, the expected minimum of Cycle 24. The linear relation obtained between the polar field and the HMF (equation 1) implies that the HMF will drop to be 4.0 ± 0.6 nT by ~2020. The error of 0.6 was estimated using standard formula for propagation of errors.

Cliver and Ling (2011) reported a strong correlation (see Fig. 2 in Cliver and Ling (2011)) between the peak values of sunspot numbers smoothed over 13-month period (SSN_{max}) and the HMF at solar cycle minimum given by equation 2.

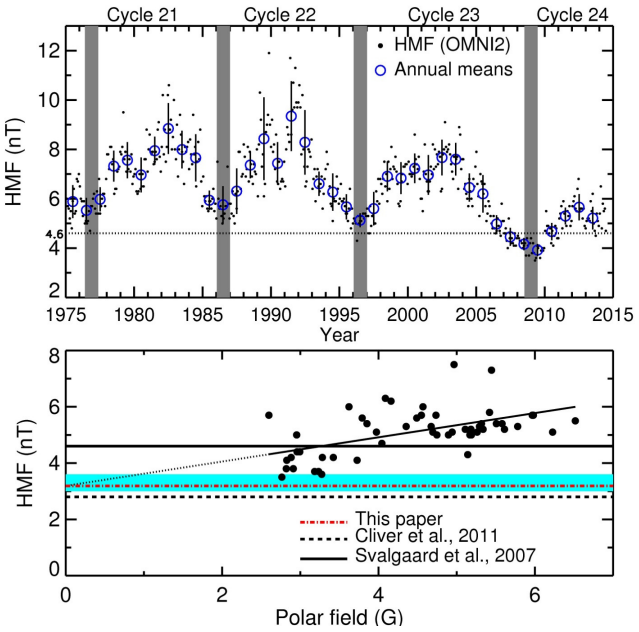

Figure 4. The upper panel shows, by solid black filled dots, measurements of the heliospheric magnetic field from the OMNI2 data base at 1 AU obtained between 1975 and 2014. The open blue circles are annual means with 1σ error bars. The horizontal line is marked 4.6 nT. The vertical grey bands demarcate 1 year intervals around the minima of solar cycles 20, 21, 22 and 23. The lower panel shows a plot of the polar field (B_p), as a function of the HMF for values during 1 year intervals around the minima of cycles 20, 21, 22 and 23. The solid black and dashed black horizontal lines indicate the floor levels of the HMF,derived by other researchers, of 4.6 nT, and 2.8 nT respectively, while the dotted red line is marked at 3.2 nT , the HMF floor level derived from the present work. The blue band shows the range for our derived floor value of 3.2 nT.

$$SSN_{max}=63.4 \times B_r - 184. \qquad (2)$$

Using our estimates of 4.0 nT for the HMF (B_r) in 2020, the expected minimum of Cycle 24, in the above linear relationship of SSN_{max} and B_r, the SSN_{max} in Cycle 25 can be estimated and is likely to be 69 ± 12 (the error of ±12 is a standard error of the mean estimated using peak sunspot numbers for cycles 14-24 from Cliver and Ling (2011)) which shows Cycle 25 is similar with Cycle 24 within uncertainties.

It is important to note here that as of July 1, 2015, the values of sunspot number have been revised Clette et al. (2014) by the World Data Center of Solar Index and Long Term Solar Observations (WDC-SILSO) in Belgium. It has been observed that the revised values of sunspot number are comparably higher than the sunspot number values estimated by the old method. The correlation reported by Cliver and Ling (2011) is actually based on the sunspot numbers estimated by the old method of counting sunspot numbers. We have therefore retained in this paper, the old system of sunspot number counts.

4. Solar Wind Micro-turbulence

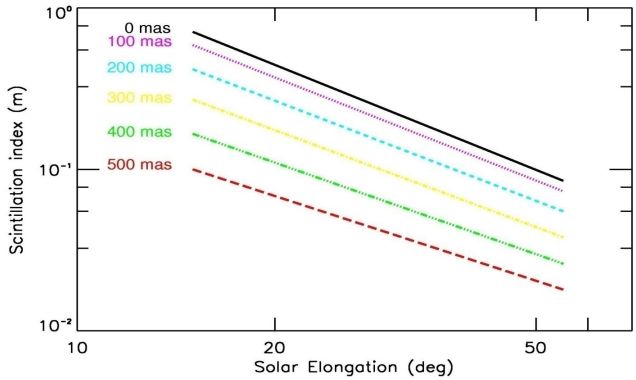

Figure 5 Marians curves of m as function of solar elongation (ε) in degree for different angular sizes of the observed source. The sources sizes, starting from the top are respectively, 0 milli arc second (mas), 100 mas, 200 mas, 300 mas, 400 mas, and 500 mas.

A study of temporal variations in solar wind micro-turbulence levels from 1983-2008, has reported a steady decline since ~1995 Janardhan et al. (2011). Another recent study, covering the solar cycle 23, of the solar wind density modulation index, $\varepsilon_N = \Delta N/N$, where, ΔN is the rms electron density fluctuations in the solar wind and N is the density, reported a decline of around 8%, Bisoi et al. (2014a) which was attributed to the declining photospheric fields. We have therefore re-examined, using IPS observations, solar wind micro-turbulence levels from between 1983-2013 to see if the declining trend has been continuing after 2008.

IPS is a phenomenon in which coherent electromagnetic radiation from extragalactic radio sources passes through the turbulent, refracting solar wind and suffers scattering. This results in random temporal variations of the signal intensity (scintillation) at the Earth (Hewish et al. (1964), which is quantified by the scintillation index (m), given by $m = \Delta S/\langle S \rangle$ where, ΔS is the scintillating flux and $\langle S \rangle$ is the mean flux of the observed source. IPS is an efficient and cost effective ground based method to study the large scale structure of the solar wind in the inner heliosphere and to track interplanetary disturbances through the interplanetary medium (Ananthakrishnan, et al., 1995; Janardhan et al., 1996; Moran et al., 2000). It is also extremely sensitive to rms electron density fluctuations ΔN_{rms} along the line-of-sight to the observed radio-source and has therefore even been used to measure enhanced scintillations through tenuous cometary tail plasma and to study extremely low density solar wind flows referred to as solar wind disappearance events (Janardhan, et al., 1991, 1992; Balasubramanian, et al., 2003; Janardhan et al., 2005, 2011).

The scintillation index drops off both with increasing heliocentric distance `r' and angular size of the radio

source being observed where, the distance of the line-of-sight (LOS) from the Sun is defined as the perpendicular distance from the Sun to the LOS of the radio source being observed. Marians (1975) effectively used a model, based on a power law distribution of the density irregularities in the weak scattering regime, to compute the theoretical values of m for radio sources of a given source size as a function of r. Figure 5 shows Marians curves for the theoretical values of m as function of the solar elongation (ε, r= Sin(ε)) for source sizes of 0 miliarc second (mas), 100 mas, 200 mas, 300 mas, 400 mas, and 500 mas, respectively. It is apparent from Fig. 5 that m is function of both distance and source size. Therefore, to study the temporal evolution of m, it is necessary to remove both the distance dependence of m and the effect of source size. In brief, the distance dependence of m can be removed by dividing each observation of m, by the corresponding m of a point source observed at the same r as described in Janardhan et al. (2011). Many years of systematic IPS observations at 327 MHz using the Ooty Radio Telescope, Manoharan (2012) have established that the strongly scintillating radio source 1148-001 has an angular size ~15 mas while VLBI observations have reported an angular diameter of 10 mas, Venugopal et al. (1985).

The effect of the source size can be removed as described in Bisoi et al. (2014a). Values of m for radio sources of a given angular size as a function of r can be computed by obtaining the theoretical temporal power spectra using Marian's coefficients, Marians (1975). The observed values of m were then normalized by finding which of the Marians curves best fitted the data for a given source. For example, the best fit Marians curve for 1148-001 corresponds to that obtained for a source size of 10 mas, an angular size estimate also corroborated by VLBI observations Venugopal et al. (1985). Since 1148-001 is a good approximation to a point source, the observed m of all other sources were multiplied by a factor equal to the difference between the best fit Marians curve for the given source and the best fit Marians curve for 1148-001, at the corresponding r. Figure 6 depicts the method of normalization of source size. The upper panel of Fig. 6 shows, by filled grey dots, the actual observations of m as a function of r for the source 0518+165. The dashed red line is the Marians curve corresponding to a source size of 10 mas, while the dashed blue line is the Marians curve which best fits to the data for the source 0518+165 (source size of 260 mas). The lower panel of Fig.6 shows the same data after it has been normalized, as described above to remove the effect of finite source size dependence.

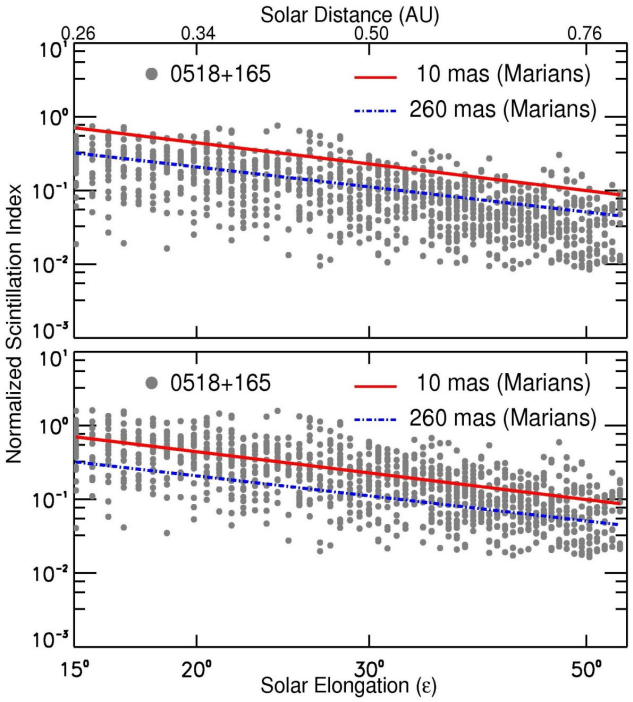

Figure 6 The upper panel shows curves of theoretical m computed using Marians model for the sources, 1148-001 (solid red line) and 0518+165 (dashed blue line). The solid grey dots are the actual measurements of scintillation indices for 0518+165. The lower panel shows observations of 0518+165 which are made source size independent by multiplying each data point by the ratio of theoretical curves of 1148-001 and 0518+165 at each ε.

After making all the observations both distance and source size independent, we shortlisted 27 sources for further analysis, each of which had at least 400 observations distributed uniformly (with no significant data gaps) over the entire range of r spanning 0.2 to 0.8 AU. Figure 7 shows, by fine black dots, the temporal variation of m for the 27 chosen sources with the large blue open circles representing annual means of m. It is evident that m continues to drop until the end of 2013. Measurements of m are basically a measure of the rms electron density fluctuations (ΔN) in the solar wind and it has been shown Ananthakrishnan et al. (1980) that solar wind micro-turbulence levels are related to both ΔN and large-scale magnetic field fluctuations in fast solar wind streams.

It is known that photospheric fields during solar minimum conditions generally provide most of the heliospheric open flux, Solanki et al. (2000). At the solar minimum the high-latitude fields extend down to low latitudes into the corona and are then carried by the continuous solar wind flow to the interplanetary space to form the interplanetary magnetic field (IMF) Schatten and Pesnell (1993). So signatures of any change in the long term behavior of photospheric fields are expected to be reflected in the IMF and solar

wind. There is thus a definite causal relationship between the photospheric magnetic fields and micro-turbulence in the interplanetary medium thereby implying that a decrease in photospheric high-latitude fields will lead to a decrease in micro-turbulence levels in the solar wind Janardhan et al. (2011). Thus, a global reduction in the long-term solar photospheric field would reflect as a corresponding decline in the solar wind micro-turbulence levels as inferred by IPS measurements. , Assuming that this declining trend continues, we have extrapolated the value of m until 2020, as indicated by a vertical red dotted line. At this point, a 10 mas source like 1148-001 will show the level of scintillation of a 160 mas source implying a reduction of approximately 30% in the solar wind micro-turbulence levels. The solid red line in Fig. 7 is the best fit to the measurements of m for the period 1990-2013 while the dotted red line is the extrapolation up to 2020.

5. Ionospheric foF2 Measurements

Since the F-region ionosphere is primarily produced by solar EUV radiation, ionospheric studies can be used as a sensitive indicator of solar activity. A crucial ionospheric parameter which has the potential to be used so is the critical frequency, in MHz, of the F-region (foF2), a quantity proportional to the square root of the electron number density at the height corresponding to that of maximum electron density Lukianova and Mursula (2011). We have examined the temporal variations in foF2 using continuous data in the period 1994-2014, from a digital ionosonde at an equatorial station, Trivandurm (8.5° N, 77° E, 0.5° N dip lat).

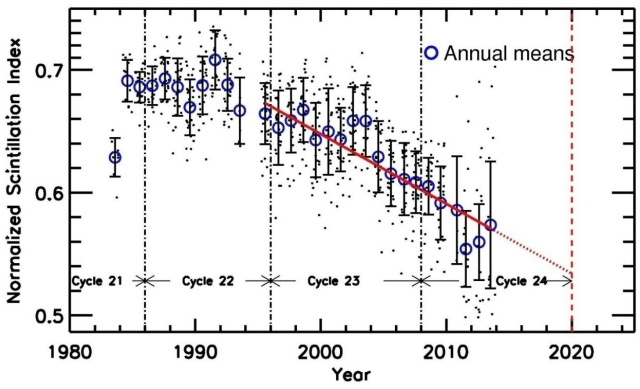

Figure 7 Shows m as function of years for observations of 27 sources after making them both source size and distance independent. While the fine dots show the actual measurements of m, the large open circles are annual means of m. The solid line is a best fit to the declining trend while the dotted line is an extrapolation to the declining trend until 2020, the expected minimum of Cycle 24, indicated by a red dashed vertical line. The black dot-dashed vertical lines demarcate solar cycles 21, 22, 23, and 24, respectively.

F-region densities show diurnal, day-day, monthly (solar rotation), seasonal, semi-annual, and annual variations. In addition, it is well known that F-region densities also exhibit solar cycle variations showing good correlation with the sunspot numbers, the latter being used as a proxy to the solar EUV radiation that is primarily responsible for the formation of the ionosphere. Over any location, the F-region densities are controlled by production, loss and transport. The role of transport is crucial and differs from location to location. If one wants to establish the dependence of solar activity represented by sunspot number alone, one should concentrate on the background representative ionization devoid of transport effects. Additionally, while using foF2 to study any long term trends, the known sources of variations should be carefully accounted for. In the present study, we have specifically used the foF2 values at 0300 LT and the choice has been arrived at from these considerations. Over the magnetic equator, only electro-dynamical processes dominate in changing the number density distribution and since these processes dominate only during the daytime and all the direct and indirect forcing reach a steady state well past midnight, over any location, and since sunrise effects are yet to be registered, it is perceived that the densities at ~0300 LT would be a good representation of the quiescent ionosphere that is directly controlled by solar activity.

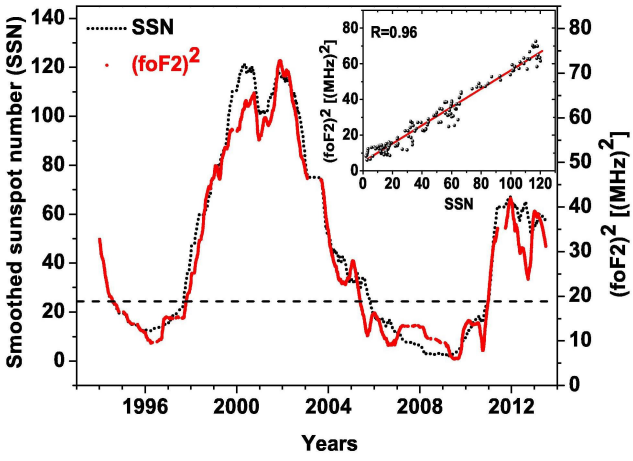

Figure 8 The correlation between the measured $(foF2)^2$ with that of the sunspot number. A thirteen month running mean, to smooth out both semi-annual and annual variations, has been applied for both parameters. A linear correlation plot between these two parameters, with a correlation coefficient of R=0.96 is shown in the inset. The horizontal dashed line is drawn at a sunspot number of 25 corresponding to a very low level of sunspot activity.

Figure 8 depicts the relation between the measured $(foF2)^2$ and sunspot number, that actually confirms the known correlation between the two. A thirteen month running average has been taken for both the parameters in order to smooth out the semi-annual and

annual variations. Shown in the inset is their correlation with a correlation coefficient of R = 0.96. Such a high degree of correlation shows that the F-region densities are very closely tied up to the solar activity represented by the sunspot number and indicates that, the maximum frequency of reflection from the F-region will be totally devoid of any long term trend as seen in the solar and interplanetary parameters. The decline in the high-latitude fields and the state of interplanetary space, which among themselves shows a great deal of similarity in their steadily declining trends, suggests a likely weak Cycle 25, and if the declining trend continues we may head towards a Maunder-like minimum.

During the previous Maunder minimum, even the existence of the ionosphere was not known, it is important to raise the question of the likely impact on the ionosphere if such a minimum is forthcoming. However, even in the complete absence of sunspots there is always a floor level of solar EUV flux which would produce a background ionospheric electron density. For example, it is known that for the years 2008 and 2009 the solar photosphere was spotless for 265 and 262 days respectively. The average $(foF2)^2$ for 2008-2009 was around 10 $(MHz)^2$, implying an ionospheric reflection cutoff at 0300 hrs LT of <3.5 MHz. By showing the very tight relation between the sunspot numbers and the representative F-region ion densities, it is demonstrated that an impending minimum is not likely to have any serious or adverse impact. However, the important message is that, unlike the decrease in solar magnetic fields and solar wind micro-turbulence indicating an impending Maunder-like minimum beyond 2020 when they become very low, the electron density of the Earth's ionosphere would always have a residual value due to the background EUV radiation. The lowering of the ionospheric cut-off frequency certainly requires further investigation by examining more data. However, this study strongly suggests that the night time ionospheric cut-off frequency is being lowered significantly thereby making ground based low frequency radio astronomy, well below 30 MHz possible.

6. Discussions and Conclusions

From our present study, based on analysis of past 39 years of solar and interplanetary observations covering solar cycles 21-24, we conclude that

1. Both solar photospheric fields and solar wind micro-turbulence levels have been steadily declining from ~1995 and that the trend is likely to continue at least until the minimum of cycle 24 in 2020.
2. The HMF, based on the correlation between the high-latitude magnetic field and the HMF at the solar minima, is expected to decline to a value of ~4.0 (±0.6) nT by 2020.
3. The peak 13 month smoothed sunspot number of Cycle 25 is likely to be ~69 ± 12, thereby making Cycle 25 a slightly weaker cycle than Cycle 24 and only a little stronger than the cycle preceding the Maunder Minimum and comparable to cycles in the 19th century.

Another study by Upton and Hathaway (2014) based on the expected behavior of the axial dipole moment after polar reversal in Cycle 24, reported that Cycle 25 will be similar to Cycle 24. There are studies that show that the peak sunspot number prior to the onset of the Maunder minimum was around 50 Eddy, (1976). Our study, which shows a decline in both the high-latitude fields and the micro turbulence levels in the inner-heliosphere since 1995, which among themselves shows a great deal of similarity in their steadily declining trends, thus begs the question as to whether we are headed towards a Maunder-like grand minimum beyond Cycle 25?

It may be noted that, a recent study Zolotova and Ponyavin (2014), reported that the solar activity in Cycle 23 and that in the current Cycle 24 is close to the activity seen on the eve of the Dalton and Gleissberg-Gnevyshev minima, and claimed that a Grand Minimum may be in progress. Also, a recent analysis of yearly mean sunspot-number data covering the period 1700 to 2012 showed that it is a low-dimensional deterministic chaotic system Zachilas and Gkana (2015). Their model for sunspot numbers was able to successfully reconstruct the Maunder Minimum period and they were hence able to use it to make future predictions of sunspot numbers. Their study predicts that the level of future solar activity will be significantly decreased leading us to another prolonged sunspot minimum lasting several decades. Our study on the other hand, using an entirely different approach, also suggests a long period of reduced solar activity.

Modeling studies of the solar dynamo invoking meridional flow variations over a solar cycle have successfully reproduced the characteristics of the unusual minimum of sunspot cycle 23 and have also shown that very deep minima are generally associated

with weak polar fields Nandy et al. (2011). Attempts to model grand minima, seen in ~11000 years of past sunspot records using ^{14}C data from tree rings (Choudhuri and Karak, 2012; Karak and Choudhuri, 2013) have found that gradual changes in meridional flow velocity lead to a gradual onset of grand minima while abrupt changes lead to an abrupt onset. In addition, these authors have reported that one or two solar cycles before the onset of grand minima, the cycle period tends to become longer. It is noteworthy that surface meridional flows over cycle 23 have shown gradual variations from 8.5 m s^{-1} to 11.5 m s^{-1} and 13.0 m s^{-1}, Hathaway and Rightmire (2010) and cycle 24 started ~1.3 years later than expected. There is also evidence of longer cycles before the start of the Maunder and Spörer minimum, Miyahara et al. (2010). It may also be noted that the current cycle 24 is already weak and our analysis suggests a similar weak cycle 25. All these indicate that a grand minimum akin to a Maunder like minimum may be in progress.

Since sunspots in conjunction with the polar field, modulates the solar wind, the heliospheric open flux and the cosmic ray flux at earth (Wang et al., 2009; Solanki et al., 2000; Lara et al., 2005), an impending long, deep solar minimum is likely to have a terrestrial impact in terms of climate and climate change. Once the interplanetary magnetic field goes through a low, it would modulate the flux of galactic cosmic rays (GCR) that arrive at the earth and there exists positive evidence for GCR's to act as cloud condensation nuclei thus enabling precipitation of rain bearing clouds (Carslaw et al., 2002; Gray et al., 2010). So the rain fall is likely to be impacted, though it would be very difficult to quantify this change. Such observations suggest that a cosmic ray-cloud interaction may help explain how changes in solar output can produce changes in the Earth's climate. However, our observations of a significant correlation between the night time F2-region electron density and sunspot number show no such declining trend for the former. This indicates that even in the impending solar quiet phase when there will be little/no sunspots, the reduced F-region electron density will, being in phase with solar activity (solar EUV radiation), give rise to a reduced ionospheric reflection cut-off frequency. In general, a reduced sunspot count will have no adverse effect on ionospheric processes including large scale atmospheric current systems.

It is for the first time such an assessment has become possible using ionospheric data as the existence of the ionosphere itself was not known during the previous grand solar minimum. It is known that F-region densities go through a solar like cycle and are low during low solar activity. Our data indicate that these would be at their lowest during an impending minimum (represented by the intercept in the inset of Figure 7) that would stay for an extended period of several years. Currently the lowest observing frequencies in India are 40 MHz for solar studies Kishore et al. (2014) and 150 MHz extra-galactic studies Bisoi et al. (2011). Our results establish that such prolonged low levels of night time F-region electron densities will open up the low-frequency radio window and be a boon to radio astronomy for ground based studies of the high red-shift radio universe well below 10 MHz.

Acknowledgments

This work was supported in part by JSPS Core-to-Core Program (B. Asia-Africa Science Platforms), Formation of Preliminary Center for Capacity Building for Space Weather Research and International Exchange Program of National Institute of Information and Communication Technology (NICT). This work utilizes SOLIS data obtained by the National Solar Observatory (NSO) Integrated Synoptic Program (NISP), operated by the Association of Universities for Research in Astronomy (AURA), Inc. under an agreement with the NSF, USA. IPS observations were carried out under the solar wind program of STEL, Nagoya University, Japan and the authors would like to thank Tokumaru, M., and Fujiki, K. for providing the IPS observations. The ionosonde data was provided by Space Physics Laboratory (SPL), VSSC, Trivandurm, India. RS and LJ duly acknowledge NASI, Allahabad for support. SA acknowledges an INSA senior scientist fellowship.

References

Ananthakrishnan, S., Coles, W. A. and Kaufman, J. J.: 1980, J. Geophys. Res., Space Physics 85, 6025, doi:10.1029/JA085iA11p06025.

Ananthakrishnan, S., Balasubramanian, V. and Janardhan, P.: 1995, Space Sci. Rev., 72, 229-232, doi:10.1007/BF00768784.

Balasubramanian, V., Janardhan, P., Srinivasan, S.and Ananthakrishnan, S.: 2003, J. Geophys. Res. Space Physics, 108, 1121, doi:10.1029/2002JA009516.

Bisoi, S. K., Ishwara-Chandra, C. H., Sirothia, S. K. and Janardhan, P.: 2011, J. Astro. Astron., 32, 613, doi:10.1007/s12036-011-9116-2.

Bisoi, S. K., Janardhan, P., Ingale, M., Subramanian, P., Ananthakrishnan, S., Tokumaru, M. and Fujiki, K.: 2014a, Astrophys. J., 795, 69, doi:10.1088/0004-637X/795/1/69.

Bisoi, S. K., Janardhan, P., Chakrabarty, D., Ananthakrishnan, S. and Divekar, A.: 2014b, Sol. Phys., 289, 41–61, doi:10.1007/s11207-013-0335-3.

Carslaw, K. S., Harrison, R. G. and Kirkby, J.: 2002, Science, 298, 1732, doi: 10.1126/science.1076964.

Charbonneau, P.: 2010, Living Rev. Sol. Phys., 7, 3,doi:10.12942/lrsp-2010-3.

Choudhuri, A. R., Chatterjee, P. and Jiang, J.: 2007, Phys. Rev. Lett., 98, 131103, doi:10.1103/PhysRevLett.98.131103.

Choudhuri, A. R. and Karak, B. B.: 2012, Phys. Rev. Lett., 109, 171103,doi:10.1103/PhysRevLett.109.171103.

Clette, F., Svalgaard, L., Vaquero, J.M. and Cliver, E. W: 2014, Space Sci. Rev., 186 (1-4), 35-103, doi: 10.1007/s11214-014-0074-2.

Cliver, E. W. and Ling, A. G.: 2011, Sol. Phys., 274, 285–301, doi: 10.1007/s11207-010-9657-6.

Connick, D. E., Smith, C. W. and Schwadron, N. A.: 2011, Astrophys. J., 727, 8,doi:10.1088/0004-637X/727/1/8.

de Toma, G.: 2011, Sol. Phys., 274, 195–217, doi:10.1007/s11207-010-9677-2.

Eddy, J. A.: 1976, Science, 192, 1189, doi:10.1126/science.192.4245.1189.

Goelzer, M. L., Smith, C. W. and Schwadron, N. A.:2013, J. Geophys. Res., Space Physics 118, 7525–7531, doi:10.1002/2013JA019404.

Gray, L. J., Beer, J., Geller, M., et al.: 2010, Rev. Geophys., 48, 4001, doi: 10.1029/2009RG000282.

Hathaway, D. H. and Rightmire, L.: 2010, Science, 327, 1350, doi:10.1126/science.1181990.

Hewish, A., Scott, P. F. and Wills, D.: 1964, Nature, 203, 1214, doi:10.1038/2031214a0.

Janardhan, P., Alurkar, S.K. Bobra, A.D. and Slee, O.B.:1991, Aus. Jou. Phys. 44 (5), 565-572.

Janardhan, P., Alurkar, S.K. Bobra, A.D., Slee, O.B. and Waldron, D.:1992, Aus. Jou. Phys., 45(1), 115-126.

Janardhan, P., Balasubramanian, V., Ananthakrishnan, S. and Dryer, M.: 1996, Sol. Phys. 166 (2), 379-401, doi:10.1007/BF00149405.

Janardhan, P., Fujiki, K., Kojima, M., Tokumaru, M. and Hakamada, M.: 2005, J. Geophys. Res., Space Physics 110, A08101, doi:10.1029/2004JA010535.

Janardhan, P., Bisoi, S. K. and Gosain, S.: 2010, Sol. Phys., 267, 267, doi: 10.1007/s11207-010-9653-x.

Janardhan, P., Bisoi, S. K., Ananthakrishnan, S., Tokumaru, M. and Fujiki, K.: 2011, Geophys. Res. Lett., 382, 20108, doi:10.1029/2011GL049227.

Jian, L. K., Russell, C. T. and Luhmann, J. G.: 2011, Sol. Phys., 69, doi: 10.1007/s11207-011-9737-2.

Karak, B. B. and Choudhuri, A. R.: 2013, Res. Astron. Astro., 13, 1339, doi:10.1088/1674-4527/13/11/005.

Kishore, P., Kathiravan, C., Ramesh, R., Rajalingam, M. and Barve, I. V.:2014, Sol. Phys., 289, 3995-4005,doi: 10.1007/s11207-014-0539-1.

Lara, A., Gopalswamy, N., Caballero-L´opez, R. A., et al.: 2005, Astrophys. J., 625, 441, doi: 10.1086/428565.

Livingston, W., Penn, M. J. and Svalgaard, L.: 2012, Astrophys. J., 757, L8, doi:10.1088/2041-8205/757/1/L8.

Lukianova, R. and Mursula, K.: 2011, J. Atmos. Sol. Terrestrial Phys., 73, 235, doi:10.1016/j.jastp.2010.04.002.

Manoharan, P. K.: 2012, Astrophys. J., 751, 128, doi:10.1088/0004-637X/751/2/128.

Marians, M.: 1975, Radio Science, 10, 115, doi:10.1029/RS010i001p00115.

Miyahara, H., Kitazawa, K., Nagaya, K., et al.: 2010, Journal of Cosmology, 8, 1970.

Moran, P.J., Ananthakrishnan, S., Balasubramanian, V., Breen, A.R., Canals, A., Fallows, R.A., Janardhan, P., Tokumaru, M. and Williams, P.J.S.:2000, Annales Geophysicae, 18 (9), 1003-1008, doi:10.1007/s00585-000-1003-0.

Munoz-Jaramillo, A., Sheeley N. R., Zhang, J. and DeLuca, E. E.: 2012, Astrophys. J., 753, 146, doi:10.1088/0004-637X/753/2/146.

Nandy, D., Munoz-Jaramillo, A.and Martens, P. C. H.: 2011, Nature, 471, 80-82, doi:10.1038/nature09786.

Petrie, G. J. D.: 2012, Sol. Phys., 281, 577, doi:10.1007/s11207-012-0117-3.

Schatten, K.: 2005, Geophys. Res. Lett., 32, 21106, doi:10.1029/2005GL024363.

Schatten, K. H. and Pesnell, W. D.: 1993, Geophys. Res. Lett., 20, 2275, doi:10.1029/93GL02431.

Smith, E. J. and Balogh, A.:2008, Geophys. Res. Lett., 35, L22,103, doi:10.1029/2008GL035345.

Solanki, S. K., Schussler, M. and Fligge, M.: 2000, Nature, 408, 445, doi:10.1038/408445a.

Svalgaard, L. and Cliver, E. W.:2007, Astrophys. J., 661, L203–L206, doi:10.1086/518786.

Svalgaard, L., Cliver, E. W. and Kamide, Y.: 2005, Geophys. Res. Lett., 32, 1104,doi:10.1029/2004GL021664.

Upton, L. and Hathaway, D.H.: 2014, Astrophys. J., 780, 5, doi:10.1088/0004-637X/780/1/5.

Usoskin, I. G., Solanki, S.K. and Kovaltsov, G.A.: 2007, Astron. Astrophys., 471, 301–309, doi:10.1051/0004-6361:20077704.

Venugopal, V. R., Ananthakrishnan, S., Swarup, G., Pynzar, A. V. and Udaltsov, V. A.:1985, Mon. Not. R. Astron. Soc., 215, 685.

Wang, Y.-M.and Sheeley Jr., N.R.:2013, Astrophys. J., 764,90, doi:10.1088/0004-637X/764/1/90.

Wang, Y.-M., Robbrecht, E. and Sheeley, Jr., N. R.: 2009, Astrophys. J., 707, 1372, doi:10.1088/0004-637X/707/2/1372.

Zachilas, L. and Gkana, A.: 2015, Sol. Phys., 290, 1457–1477,doi: 10.1007/s11207-015-0684-1.

Zolotova, N.V. and Ponyavin, D.I.:2014, J. Geophys. Res., Space Physics 119, 3281–3285, doi: 10.1002/2013JA019751.